BEAM-BASED OPTIMIZATION OF STORAGE RING NONLINEAR BEAM DYNAMICS *

Xiaobiao Huang†, James Safranek, SLAC, Menlo Park, CA 94025, USA

Abstract

This paper will present considerations and algorithms for direct online optimization of the nonlinear beam dynamics of existing and future storage rings. The experimental setup and results from using this approach to improve the dynamic aperture of the SPEAR3 storage ring, using the robust conjugate direction search method and the particle swarm optimization method, will be covered.

INTRODUCTION

Storage Ring Nonlinear Beam Dynamics Challenges

A storage ring is a complex machine with high demand of precision over its sub-systems. In particular, alignment and magnetic field of all magnets have to meet stringent tolerance requirements for the machine to work. Even with such precision, the machine as built is generally not going to reproduce the design completely. Residual errors will add up and further compound the deviation.

To the zero'th order, the magnetic field errors cause orbit distortions, which can be corrected with orbit correctors relatively easily. The first order magnetic field errors cause errors to the linear optics as represented by beta beating and betatron phase advance beating. Linear optics errors can be corrected with beam based methods such as LOCO [1–3] and ICA-TBT [4, 5].

Errors from higher order magnetic fields are nonlinear perturbation to the beam motion. They will cause deviations of the nonlinear beam dynamics behavior from the ideal design model and typically result in poorer nonlinear beam dynamics performance, in terms of reduced dynamic aperture and momentum aperture. As an illustration, we write down the nonlinear perturbation terms to the Hamiltonian for an on-energy particle

$$H_1 = \sum_{jklm\geq 0} \sum_{p} h^{(p)}_{jklm} J_x^{\frac{j+k}{2}} J_y^{\frac{l+m}{2}} e^{i[(j-k)\phi_x+(l-m)\phi_y+p\theta]}, \quad (1)$$

where $J_{x,y}$ are action variables, $\phi_{x,y}$ phase variables and $\theta = s/R$ is the free variable, and $h^{(p)}_{jklm}$ are integrals of the magnetic field errors, powers of beta functions, and corresponding phase factors over the circumference. For off-energy particles, there are yet more nonlinear resonance terms associated with the energy errors.

Terms in Eq. 1 with $j = k$ and $l = m$ cause betatron tune shifts with amplitude. Other terms drive resonances

$$(j-k)\nu_x + (l-m)\nu_y + p = 0.$$

As the tunes of an oscillating beam shift across certain resonance lines (or intersections of two or more resonance lines), beam motion can become chaotic and eventually lead to beam loss. This is essentially how nonlinear beam dynamics limit the dynamic aperture and local momentum aperture. The magnetic field errors and residual linear optics errors (after correction) will alter the strengths of the $h^{(p)}_{jklm}$ coefficients, which in turn will change the beam tune footprint and the strengths of the the resonance driving coefficients. The performance limiting resonances may not be the same for a different set of errors. Therefore, storage ring nonlinear beam dynamics is generally a complicated problem to tackle.

Methods of compensating machine errors for performance improvement may be classified to two categories: beam based correction (BBC) and beam based optimization (BBO) [6]. Beam based correction requires an ideal target condition, diagnostics that detect the deviations of the actual machine from the target, and a deterministic approach to find the corrections. For nonlinear beam dynamics, the requirements of BBC are not easily met. The main difficulty is that there is no diagnostics to provide credible information for correction.

The nonlinear dynamics correction methods explored so far typically use amplitude-dependent and chromatic tune shifts [8], and/or measured resonance driving terms (RDTs) [7, 9, 10] as representation of the nonlinear dynamics behavior of the machine. These measurables are then fitted to the ideal model to obtain corrections. We note that the measured tune shifts are the total effects of contributions from many $h^{(p)}_{jklm}$ terms; thus the actual distribution of errors around the ring or over the $(jklm)$ coefficients cannot be resolved.

Measurement of the RDTs is usually difficult because it requires precise knowledge of the linear optics and typically there is no strong signals on the resonance tunes. Even though recent studies have demonstrated measurements of up to octupolar RDTs [9], it remains unclear if the correction of such RDTs necessarily leads to an improvement of nonlinear dynamics, given the complexity of the underlying process. In fact, the ESRF study cited above reported that an RDT correction led to a reduction of beam lifetime [11].

Because of the intrinsic difficulty of BBC for nonlinear dynamics, we believe the solution may be beam based optimization.

BBO for Nonlinear Neam Dynamics

Unlike BBC, BBO does not require an ideal model or sophisticated diagnostics to detect the deviation from the model. Instead, the machine is used as a function evaluator to directly optimize the nonlinear dynamics performance - in terms of dynamic aperture or Touschek lifetime. The key

* Work supported by DOE Contract No. DE-AC02-76SF00515
† xiahuang@slac.stanford.edu

component of BBO is efficient, robust optimization algorithms that work for noisy functions.

At SPEAR3 we have developed BBO algorithms and applied them to many practical accelerator problems [12, 13]. An important application is the nonlinear beam dynamics optimization of the SPEAR3 ring. This work has been reported in Ref. [13]. In the following we will give a brief summary of the study, provide supplemental information, and describe new development since then.

SPEAR3 NONLINEAR BEAM DYNAMICS OPTIMIZATION

Experimental Setup

SPEAR3 is a third generation light source with a beam energy of 3 GeV. It currently has a horizontal emittance of 10 nm. Since 2011 we have worked on developing a new lattice to reduce the emittance to below 7 nm. A critical component of the study is to achieve the nonlinear beam dynamics performance. In simulation we found that by breaking up the Standard cell sextupoles from two serial power supplies to eight smaller groups, the additional degrees of freedom allow simultaneous optimization of dynamic aperture and momentum aperture.

In 2014 new sextupole power supplies were added. There are a total of 10 sextupole power supplies, 5 for focusing sextupoles, and 5 for defocusing sextupoles. The grouping of these sextupoles follow symmetric patterns around the ring, as illustrated in Figure 1.

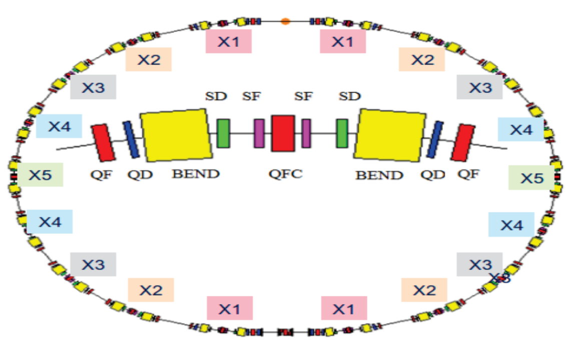

Figure 1: Layout of SPEAR3 sextupole families.

Since all sextupoles are located in dispersive region, a change of a sextupole knob generally will change the chromaticities. To get the maximum degrees of freedom in optimization, we used combined knobs as defined by the null space of the chromaticity response matrix [13]. The eight free knobs are shown in Figure 2.

The SPEAR3 10-nm lattice normally has sufficient dynamic aperture for the injected beam. In the optimization experiment we first reduce the kicker bump. This effectively increases the dynamic aperture requirement. An illustration of the relation ship of the dynamic aperture, kicker bump, and stored beam to injection beam separation is in Figure 3.

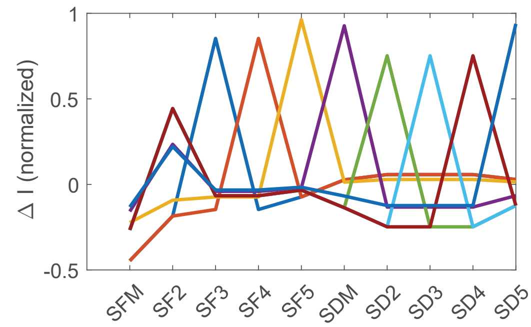

Figure 2: Chromaticity independent sextupole knobs for SPEAR3.

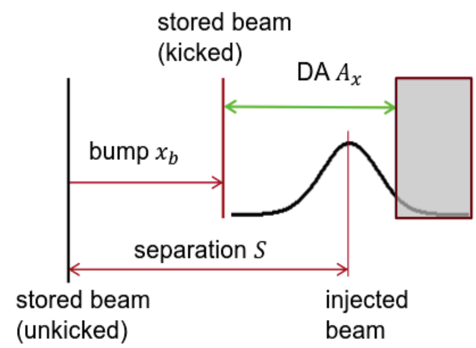

Figure 3: Injection and kicker bump.

The optimization objective function is the injection efficiency. To obtain a stable, low noise measure of injection efficiency, we monitor injection for 10 seconds and use the stored beam current increment to divide the average injector beam in the same 10 seconds. The resulting injection efficiency function still has a noise sigma of $\sim 3\%$.

Optimization Algorithms

Two online optimization algorithms have been used in the SPEAR3 nonlinear dynamics study, the robust conjugate direction search (RCDS) algorithm [12] and the particle swarm optimization (PSO) algorithm [14, 15].

The RCDS algorithm was designed for online optimization. It uses a novel robust 1-D optimizer to search multiple directions iteratively. In this study, since the knobs are simply the basis of the chromaticity response matrix null space, the directions are not mutually conjugate for the dynamic aperture optimization problem. However, it still demonstrated high efficiency in finding high injection efficiency solutions. Typically in one or two iterations we can find sextupole solutions with substantially better performance.

The PSO algorithm is a stochastic optimization method. It creates new solutions by following the trajectories of a population of moving "particles" in the parameter space. The trajectory is affected by the global best solutions and the best solution in the particle's history. We use the same algorithm control parameters as in Ref. [15]. In general the PSO is not as efficient as RCDS. But because of its stochastic nature, it has the potential to jump out of a local attractor and converge to the global optimum. In our experiments PSO is launched from the vicinity of an optimized solution found by RCDS.

Experimental Results

As is shown in Ref. [13], starting from the flat sextupole configuration (nominal setting before 2014), the RCDS found an optimized solution in less than 250 function evaluations. Starting from a previously optimized solution (w/ RCDS), PSO found a better solution within less than 300 evaluations. The solutions found by RCDS and PSO have similar patterns in sextupole set-points. The dynamic aperture was measured to be significantly increased for both solutions, by more than 5 mm. The dynamic aperture increase was confirmed with injection measurements with reduced injection kicker bump.

The Touschek lifetime for the optimized solution was slightly lower only because the coupling ratio was changed during optimization. In later experiments the coupling was made equal with the flat sextupole solution and the lifetime was measured to be almost identical. Lifetime vs. RF gap voltage measurements also indicated that there was no reduction of local momentum aperture.

RECENT PROGRESS AT SPEAR3

DA Optimization for High Vertical Chromaticity

The addition of a new in-vacuum undulator (for BL15) has caused operation difficulty as at high current the beam can drive a resonant electromagnetic mode in this device which then drives vertical coupled bunch instability. It has been found that increasing vertical chromaticity to above +6 can suppress this mode. However, when the sextupoles were changed by equal amounts for SF and SD families, respectively, from the sextupole solution optimized for $(C_x, C_y) = (+3, +3)$ to increase C_y, the dynamic aperture became worse. The dynamic aperture got worse also when C_y was reduced from +3 (see Figure 4). Clearly, it is not the increase of sextupole strength, but the deviation from the optimized solution that caused the DA reduction.

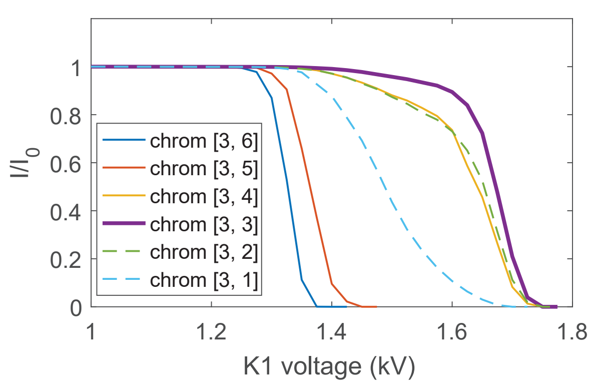

Figure 4: Dynamic aperture measurement for various vertical chromaticity values. The solution was optimized for $C_y = 3$. The K1 calibration is 1.212 mrad/kV.

This observation prompted us to optimize DA for the elevated vertical chromaticity case with $C_y = 5$. Starting from the (+3, +5) case shown in Figure 4, we ran RCDS for only one iteration and found a better solution. The DA measurement for the new solution is compared to the original ones in Figure 5. DA for the optimized solution (w/ $C_y = 5$) is similar to the $C_y = 3$ case before optimization. And, incidentally, when vertical chromaticity is increased to $C_y = 6$, the DA is slightly better. This solution is suitable for high chromaticity operation.

The sextupole set-points (in terms of changes from the flat sextupole pattern) for the (3, 3) before optimization, the (+3, +5) solutions before and after optimization are compared in Figure 6. The differences are mainly in the SD magnets, especially SD2 and SD5.

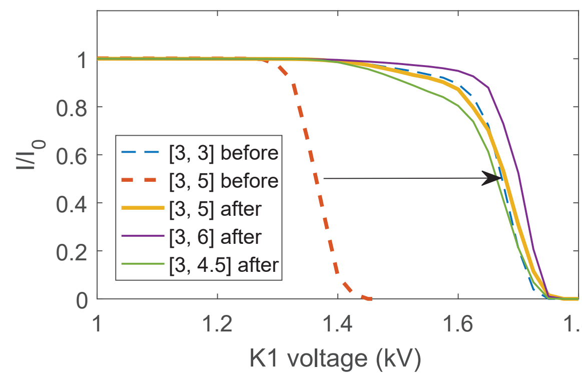

Figure 5: Comparison of dynamic aperture measurement before and after optimization for the (3, 5) case.

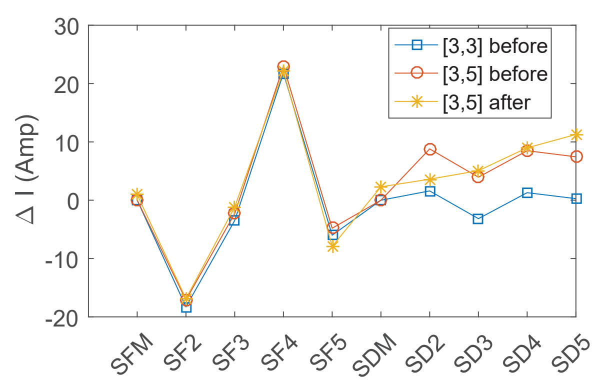

Figure 6: Sextupole changes from flat sextupole pattern before and after the optimization for the $C_y = 5$ case.

DA Optimization w/ a Long-period EPU

The sextupole solution optimized for chromaticities of (3, 3) was done with BL5 EPU at its nominal gap of 40 mm. This is an EPU with strong field, and long period (λ_u = 140 mm). Because the dynamic kick from the horizontal field roll off is proportional to λ_u^2, the device has very strong nonlinear dynamics impact to the beam. Recently in operation, as the BL5 EPU is closed to 13.4 mm in the circular EPU phase (the circular phase is the worst for this

ISBN 978-3-95450-182-3

device in terms of dynamics impact), the injection efficiency had a significant drop, to 75%.

Measurements of dynamic aperture with BL5 gap at the nominal value and the minimum value (12.6 mm) showed a significant difference. Probably the recent sextupole solution is more sensitive to BL5 EPU perturbation because previously (before December 2016) we did not observe such a big injection efficiency decrease. We then did DA optimization using RCDS with BL5 EPU at the minimum gap and the circular phase. The algorithm found a solution that is much less susceptible to BL5 gap changes. The new solution is more suitable for operation since it has no injection efficiency reduction with BL5 gap closed to minimum value. The measured DA for BL5 at nominal or minimum gap values before and after this optimization is shown in Figure 7. The sextupole changes are shown in Figure 8.

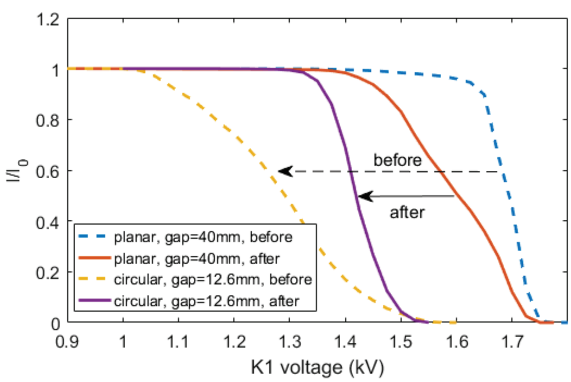

Figure 7: DA w/ BL5 EPU open or close, before and after the optimization with gap closed.

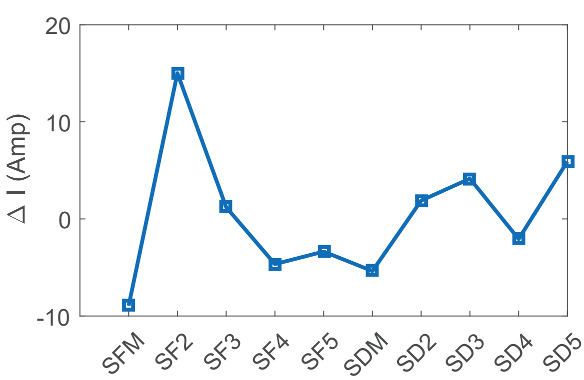

Figure 8: Sextupole changes by the DA optimization with BL5 gap closed.

BEAM LIFETIME OPTIMIZATION

In addition to dynamic aperture, adequate momentum aperture for acceptable Touschek lifetime is another important nonlinear beam dynamics performance requirement. At the SPEAR3 the momentum aperture is mostly determined by the RF bucket height, not nonlinear beam dynamics.

At ESRF, beam lifetime optimization has been successfully carried out with the RCDS method [16]. In the experiments the objective function was beam lifetime normalized by measured vertical beam size, beam current, and calculated bunch lengthening. In separate tests, 12 sextupole correctors or 10 main sextupole variables were used as knobs. Substantial lifetime increase was obtained for both tests. For the case with sextupole correctors it took about 300 function evaluations to reach the optimum. The optimized sextupole solution was used for operation and had several important benefits.

SUMMARY

We have proposed to use online optimization to realize or exceed the design performance for storage ring nonlinear beam dynamics. Using the online optimized algorithms developed at SPEAR3, we have successfully demonstrated the effectiveness of this approach in dynamic aperture for the SPEAR3. Touschek lifetime optimization with the same method has been demonstrated at ESRF.

REFERENCES

[1] J. Safranek, Nucl. Instr. Meth. A, 388 (1-2) (1997) 27.

[2] G. Portmann, J. Safranek, X. Huang, ICFA Newsletter 44, 49-60 (2007).

[3] X. Huang, J. Safranek, G. Portmann, ICFA Newsletter 44, 60-69 (2007).

[4] X. Huang, S.Y. Lee, E. Prebys, R. Tomlin, Phys. Rev. ST Accel. Beams 8, 064001 (2005).

[5] X. Yang, X. Huang, Nucl. Instr. Meth. A, 828 (2016) 97-104.

[6] X. Huang, "Development and Application of Online Optimization Algorithms", in *Proc. NAPAC'16*, Chicago, IL, USA, paper FRA2IO01.

[7] R. Bartolini, I.P.S. Martin, J. H. Rowland, P. Kuske, and F. Schmidt Phys. Rev. ST Accel. Beams 11, 104002 (2008).

[8] R. Bartolini, I. P. S. Martin, G. Rehm, and F. Schmidt, Phys. Rev. ST Accel. Beams 14, 054003 (2011).

[9] A. Franchi, L. Farvacque, F. Ewald, G. Le Bec, and K.B. Scheidt Phys. Rev. ST Accel. Beams 17, 074001 (2014).

[10] J. Bengtsson, I.P.S. Martin, J.H. Rowland, and R. Bartolini Phys. Rev. ST Accel. Beams 18, 074002 (2015).

[11] A. Franchi, Presentation at LER2014, Frascati, Italy (2014).

[12] X. Huang, J. Corbett, J. Safranek, J. Wu, Nucl. Instr. Meth. A, 726 (2013) 77-83.

[13] X. Huang, J. Safranek, Phys. Rev. ST Accel. Beams 18, 084001 (2015).

[14] X. Pang, L. Rybarcyk, Nucl. Instr. Meth. A 741, 124 (2014).

[15] X. Huang, J. Safranek, Nucl. Instr. Meth. A 757, 48 (2014).

[16] S. M. Liuzzo, N. Carmignani, L. Farvacque, B. Nash, T. Perron, P. Raimondi, R. Versteegen, S. M. White, "RCDS Optimizations for the ESRF Storage Ring", in *Proc. IPAC'16*, Busan, Korea, May 2016, paper THPMR015, pp.3420-3423.